MODEL INTERPRETATION OF CLIMATE SIGNALS: AN APPLICATION TO THE ASIAN MONSOON CLIMATE

William K. M. Lau
NASA Goddard Space Flight Center
Greenbelt MD

October 2002

(Contribution to Chapter 9 of book "The Global Climate System: Patterns, Processes, and Teleconnections" Cambridge University Press)

1. Introduction

Numerical modeling is a powerful tool to provide better understanding of the *modus operandi,* and the prediction of the earth's climate system. However, a climate model's usefulness is limited by its crude representations of physical processes, most of which we do not understand very well. Since models are only crude approximation of the real system, model results must be validated against observations to ensure reliability. The scarcity of detailed observations for climate processes with the high spatial and temporal resolutions needed for model validation and improvement has been a major impediment for improvement in climate model simulation capability and model predictions.

Climate modeling is an attempt to mimic the evolution of the real climate states, which are described by a vast set of long-term global and regional observations in the atmosphere, ocean and land, from both *in situ* and satellite observations. Given that there are large uncertainties both in observations and in models, and that even the best model is simply a crude approximation of the real world, models and observations should be used in a synergistic manner for better understanding and for improved prediction. The relationship between observations, climate models, data assimilation, process studies and climate predictions are shown schematically in Fig. 1. A climate model consists of a dynamical core represented by governing equations of climate state variables, and physics modules of varying complexity (see next section for further discussion). The physical modules, which appeared in the form of numerical sub-models or parameterizations are the drivers of a climate model. The modules are developed and continuously improved from knowledge gained from field measurements and related process studies. Long-term monitoring refers to observations that are made repeatedly for sustained periods to track the evolution of key parameters of the earth system. Because models are imperfect, and observations have inherent errors and inadequate coverage, neither model nor observations alone will provide a full, comprehensive description of the earth's climate system. For such a description, data assimilation plays a critical role. Data assimilation is the numerical process by which observations are assimilated into models to produce a complete set of dynamically consistent data set for the entire climate system (Kalnay et al 1996). Climate predictions can be derived either from observations

through statistical techniques or from climate models, or combination i.e., statistical-dynamical predictions. Data assimilations can provide model with appropriate initial states to produce more skilful predictions.

<Insert Fig. 1>

In this Chapter, we address the various issues arising from using models for detecting, understanding and predicting climate signals. This chapter consists of two main parts. The first part is devoted to discussions of climate models as a tool for climate studies, including a brief history of the development of climate models, model basics, and modeling methodologies used in modeling studies. The second part is an illustration of the use of climate models to study the anomalous climate of the Asian monsoon.

2. A climate model Primer

2.1 A brief history

Climate models originate from atmospheric general circulation models (AGCM) used in numerical weather forecasting. AGCMs for numerical weather forecasting were developed during the 1950–60s. (Charney et al. 1950, Smagorinsky et al., 1965, Bengtsson and Simmons 1983). By the early 1970's most weather services around the world have adopted numerical weather predictions model for short-term (days) to medium range (weeks) weather forecast. During that period, climate modelers first began to explore the use AGCM to study climate anomalies through numerical experimentations with various prescribed forcing functions in the atmosphere, land and oceans (Manabe and Wetherald 1975, Manabe et al 1979, Gilchrist A., 1977, 1981). A climate model differs from a weather prediction model in that the former has to be integrated for extended period of time (multi-years), where the latter is generally integrated for a few days at the most. Some of the current climate models to study global change have carried out integration up to thousands of simulated years in order to determine the reliability of long-term climate signals. Because of requirement for long-term integration, climate models are most sensitive to the conservations of mass, energy and moisture. Small imbalance in any of the conservation properties can introduce

substantial errors that may amplify during the course of the integration to produce severe model systematic bias - a problem known as "climate drift". In contrast, for numerical weather prediction, the accuracy of the initial conditions is more critical, and simulations generally cover a period too short for the climate drift to be an issue.

One of the problems facing the climate modeling community in the 70's-80's has been the enormous demand on computation resources required to carry out long-term climate simulations. As a result, for most early applications, climate models with coarse resolutions of order of 250- 500 km, with 2-10 vertical layers, were used and the simulation periods limited to a few years (Rowntree 1972, Manabe et al. 1981, Shukla and Wallace 1983, Sud and Fennessy 1982 and many others). At such coarse resolution, many physical processes are grossly under-represented. For this reason, many of the early climate model results can only be regarded as mostly exploratory. With the advent of computer technology, and more efficiency computation codes, climate models can now be run at increasing spatial and temporal resolutions, and with ever more increasing complex physics modules. At present, climate models are currently being run with resolution higher than 50 km resolution at operational centers such as ECMWF. Integrations have been carried out for hundreds of years, such as those used for the IPCC climate assessments, and other global change scenarios by many climate modeling groups around the world. Currently, the Earth Simulator Project at the Frontier Global Change Research Program of Japan is running global climate models at approximately 10 km resolution, with over 200 layers in the vertical and for hundred of simulated years.

However, even with very high-resolution climate models, large uncertainties remain with regard to prediction of future climate change, especially in the projection of statistics of increased hazards in regional and sub-regional scales due to extreme weather events. This shortcoming stems from our very limited understanding of the physics of the real climate system, which makes it impossible to include all the details required at the higher model resolution. Hence, merely increasing resolution is not a panacea to the problems of climate modeling. Our knowledge of physics of the earth system still needs to catch up with the advances in computer technology. At a more fundamental level, climate signals at the regional and sub-regional scale maybe inherently chaotic and therefore unpredictable. Even if the local signals are there, climate information downscaled from

global climate models may be masked by large random local fluctuations. To unmask the regional and sub-regional scale signals from noise, a number of modeling strategies have been adopted (see discussion in Sections 2.3 and 2.4).

2.2 Elements of a climate model

A climate model is derived from atmospheric general circulation model, with a dynamical core consisting of set of primitive equations for the atmospheric state variables such as temperature, pressure, wind and water vapor, which govern the fluid motions, thermodynamics and conservation properties for fluid motions of air parcels in the troposphere and stratosphere on the rotating earth. The equations are extremely complex and can only be solved numerically on a horizontal grid system with different vertical levels (See Fig. 2).

<Insert Fig. 2>

The AGCM are coupled to components models of the oceans, the land and the biosphere. Each component model has its own governing equations for its state variables and physical processes. The grid spacing and vertical interval in the atmosphere, ocean and the land are often different because of the different fundamental spatial and temporal scales of dynamical and physical processes in each component, as shown schematically in Fig. 2. The dynamical equations are driven by physical processes which constitute the forcing functions of the climate system. These processes which are represented as physics modules, or "parameterization" include absorption and reflection of solar energy, emission of terrestrial radiation, aerosols, atmospheric composition and chemistry, latent heat release, moisture transport, processes underlying the formation of clouds, rain and water vapor, boundary layer processes, surface fluxes of heat and water, ocean salinity, temperature and currents and sea ice as well as land surface processes including soil moisture, river run-off land vegetation and biomass photosynthetic processes, and many others. Given the proper initial and boundary conditions, and external forcing functions, i.e., solar radiation, and time history of its atmospheric composition, a climate model can be integrated forward in time, starting at some time in the past up to the present to simulate past history of the earth's climate. These climate history simulations are

important to ensure that the climate models have the capability to predict future climates. Currently, climate models are routinely being run in major research institution to provide guidance for seasonal-to-interannual, i.e. El Nino and related regional climate, predictions. Under the Intergovernmental Policy for Climate Change initiative (IPCC) models have also been run for hundreds of simulated years into the future, subject to different scenarios of climate change regarding the different rate of increase of carbon dioxide in the atmosphere, to provide projection for future climates associated with global warming.

2.3 Experimental design

In a fully coupled model, all components models are interactive. In principle, once the initial and boundary conditions are specified, a climate model can be integrated indefinitely into the future, to produce the so-called "nature" or control run. Very often to test out a given hypothesis, a climate model has to be re-run with one or more components held fixed, the results compared with the control run. Table 1 shows possible configurations in which a climate model with three major components i.e. atmosphere, ocean and land, can be run to test climate sensitivity to anomalous SST forcings due to El Nino, and land surface processes.

<Insert Table 1>

In all model sensitivity or climate simulation studies, a control experiment has to be defined first. In Table 1, the control experiment (Exp-I) is one in which the SST field is prescribed as the climatology, i.e., the mean over many years. The climatological SST describes the part of variation that is due to forcings external to the climate system, i.e., annual cycle of solar radiation. Here, deviations from the climatology are due either to internal dynamics within the atmosphere and its interaction with the land surface. In the control, the model can be integrated for typically 50 simulated years to obtained a stable climatology. In Exp-II, the model is run under identical conditions as in the control, except that the SST is obtained from actual observations that cover a 50-year period which include several major El Ninos. The anomalies in Exp-II will then be computed

with respect to the control. The impacts of El Nino SST forcings on global climate can be estimated from the anomaly fields of rainfall, temperature and wind, and from comparison with the actual observations. Since it is possible that, some of the regional impacts over land may be due to land processes feedback induced by the SST. To estimate the effect of land-atmosphere interaction, results from Exp-III and Exp-I need to be analyzed. If the interest is to isolate the natural variability generated by land-atmosphere interaction alone, without SST anomaly forcings, Exp-IV should be compared to Exp-I. Finally, comparing the fully interactive run Exp-V with Exp-II will provide insight on the role of coupled ocean-atmosphere processes in producing the model climate anomalies.

An example of a set of experiments to show the effect of ocean forcings vs. land-atmosphere interactions on the generation of the Southern Oscillation (SO) is shown in Fig. 3 (Lau and Bua 1998). The SO is a east-west seesaw in surface pressure between the tropical eastern and the western hemisphere, defined by the sea level pressure difference between Darwin and Tahiti. The SO is known to have strong impacts on the Asian monsoon climate anomalies. Comparing Exp-II (ALO, in Fig. 3a) with Exp-I (AL in Fig. 3c), it can be seen that eastern portion of the seesaw is missing in the latter when the anomalous SST forcing is withheld. This suggests that the SO arises primarily from anomalous SST forcing. The similarity in the SO in Exp-III (AO in Fig.3b) with Fig. 3a implies that land-atmosphere interaction is not important in generating the SO, but may have some impact on the signal at higher latitudes. Finally, the negative anomalies over the extratropical North Pacific and the North Atlantic in Exp-III (Fig.3c) and Exp-IV (A in Fig.3d) suggest that there is an intrinsic inverse variation of the tropical and extratropical atmospheres even in the absence of any anomalous SST forcings.

<Insert Fig. 3>

If the objective has been to examine the impact of a particular land surface anomaly such as snow cover as a climate forcing, then it is possible to run a new set of experiments in which the land and ocean forcing conditions can be reversed. The design

of the numerical experiments using climate models will depend on the objectives of the experiments, and on the hypotheses being tested.

2.4 Ensemble simulations

Given that atmospheric variations have a large chaotic component, it is possible that even forced by a specified lower boundary anomaly such as SST, the atmosphere may respond differently depending on the initial conditions (Lorenz 1963). Often, the real climatic signals are obscured by the large variability due to internal dynamics of the atmosphere. Ensemble forecasts have commonly been used in numerical long-range weather forecasts since the late 1980's to extend the lead time for useful forecasts and to evaluate the skill of the forecasts using some measure of the spread among the ensemble members (Hoffman and Kalnay 1983, Palmer 1993, Tractor and Kalnay 1993). To increase the signal-to-noise ratio and to extend predictability, ensemble approaches are increasingly being used in long-term climate simulations and projections (Shukla et al. 2001, Kawamura et al.1998). Typically, an ensemble climate simulation calls for a set of control experiments and a set of anomalous experiments. Typically, the control consists of at least 5 to 10 members subject to identical climate forcings, e.g. SST, sea ice, or present-day CO_2 composition etc., but different initial conditions, to ensure the model results span the range of possible realizations of the model climate.

In the anomaly experiments, the ensemble integrations are repeated as in the control, but the forcing function is varied in some specified, but identical manner, but with different initial conditions. The sensitivity of the forcing function on the climate system can then be evaluated based on the variance of the ensemble mean and the spread of the ensemble members about the mean. For a climate variable X_{ij}, where the index, i (= 1,2....N) is the time index, say at yearly intervals, and the ensemble number, j (=1, 2... n), the ensemble mean $\overline{x_i}$ and the climatological mean $\overline{\overline{x}}$ are defined by

$$\overline{X_i} = \frac{1}{n}\sum_{j=1}^{n} X_{ij} \; ; \; \overline{\overline{X}} = \frac{1}{nN}\sum_{i=1}^{N}\sum_{j=1}^{n} X_{ij}$$

An unbiased estimator of the variance of the noise and of the ensemble is given respectively by

$$\sigma^2_{noise} = \frac{1}{N(n-1)} \sum_{i=1}^{N} \sum_{j=1}^{n} (X_{ij} - \overline{X_j})^2$$

$$\sigma^2_E = \frac{1}{N-1} \sum_{i=1}^{N} (\overline{X}_i - \overline{\overline{X}})^2$$

The climate forced variance ad the total variance is obtained respectively as

$$\sigma^2_{signal} = \sigma^2_E - \frac{1}{n} \sigma^2_{noise}$$

$$\sigma^2_{total} = \sigma^2_{noise} + \sigma^2_{signal}$$

The climate signal-to-noise ratio is then defined as $S = \frac{\sigma^2_{signal}}{\sigma^2_{total}}$. The statistical significance of the signal for a given ensemble climate experiment can then be tested using the F-test (Von Storch and Zwiers 1999). The larger the ratio, the more likely is that the signal is detectable in the real world.

In most applications, the ensemble mean is computed with equal weights for each ensemble members. In more recent applications, when the ensemble comprises not only outputs from the same models with different initial conditions, but also different models, it may be necessary to assign different weights to each model ensemble members. In the so-called multi-ensemble super-ensemble approach, weights for each model variable and for each model grid are assigned based on past model performance (Krishnamurti et al 2000, Stefanova et al 2002). In this way, models with strong biased tend to be weighted less than those with less biased. The super-ensemble approach has produced remarkable improvement in short-term weather forecasting and is promising as a tool in multi-model climate projections.

2.5 Climate Downscaling

To produce multiple realizations of climate variability and to obtain robust statistics, climate models have to be run at the fully coupled ocean-atmosphere-land

mode for many simulated years. For seasonal-to-interannual time scales, typically 40-50 simulated years are need. For decadal scales and climate change scenarios, several hundred or even thousands of simulated years have to be carried (cf. IPCC reports). Because of the enormous computation resources required for such long–term integrations, coupled models are typically run at the low-resolution mode to capture only the slow physics of the system, which are deemed to be important for long-term climate change. As a result, regional and sub-regional scale processes are unresolved. To obtain regional and local climate information from the long-term integrations, climate downscaling is necessary

<Insert Fig. 4>

Climate downscaling is the procedure by which climate signals at the scales of GCM grid size are translated into regional and subregional scales, which are unresolved by GCMs (Giorgi and Mearns 1991, Hewitson and Crane 1996). Downscaling is usually applied to a pre-selected region, in which regional climate and/or water resource assessment need to be estimated. As shown in Fig. 4, downscaling may take place in single or multiple stages. At present, there are four basic approaches: statistical, nested models, time-sliced method and variable-grid GCM. In the statistical approach, cross-scale relationships, known as "transfer functions" are first derived from large scale observational and local-scale data, and checked for consistency with the synoptic scale forcings of the GCM. For a given climate scenario provided by the low resolution GCM (typically with horizontal resolution of 250-500 km), the transfer functions are used to generate the statistics from global GCM outputs to regional scales. This approach is limited by the amount of available global and regional data required for robust statistics, and the possible inconsistency between model and observational data. It has the clear advantage of computational ease. In the nested regional model approach, the large scale forcing functions derived from the GCM are used as laterally boundary conditions to drive a regional climate model (with typical resolution of 20-50 km) applied to a specific geographic region usually of continental to sub-continental scale, and for chosen time period of interest. This time period may be related to the occurrence of a devasting

drought or flood in a certain region, and one wants to see what are the causes, and if they are related to the underlying large scale climate forcings or to local feedback processes. Multiple nesting grids, with increasing resolutions are sometimes used to zoom in on a sub-region to resolve even smaller scale features. The nested regional models may have numerical instabilities at the lateral boundaries, so that appropriate buffer zones have to be designed (Georgi and Mearns 1991).

Alternatively, to avoid the lateral boundary problems, a time-sliced approach is used, by re-running the atmospheric component of the coupled GCM, at a higher spatial resolution and for a shorter time period, using the large-scale lower boundary forcings, such as sea surface temperature, from the coupled model. This approach has the disadvantage of "wasting" valuable computational resources outside the region of interests. More recently, a new strategy has been developed to use GCM's with variable resolution, or so-called stretched or "telescoping grids" in which the GCM can zoom in on a specific region, with high resolution to resolve local features, while keeping the computations elsewhere at the coarse resolution (Fox-Rabinovitz et al. 2001). This approach can achieve considerable savings in computation resources, while achieving the desired higher spatial resolution in the region of interests. The variable-grid GC requires the re-design of the model numerics, as well as the physical parameterizations to maintain dynamical consistency between the regions with high and low resolutions.

Depending on the space-time resolutions, outputs from the regional models can be used for climate assessments, and for water resource managements. For applications to river-basin, catchment scales, further downscaling may be needed (Lattenmaier et al. 1999). For that purpose, outputs from the regional climate models are used to drive macro-scale lhydrology model (<1 km resolution) to provide information such as stream-flow, surface runoff, subsurface water storage, needed for management of irrigation, flood control, hydropower production, municipal and industrial supply, navigation and recreation.

2.6 Model Intercomparison and Validation

Given the large uncertainties in GCMs, it is clear that results from a single model cannot be interpreted too literally and that an estimate of the model reliability has to be

included. This consideration has led to the Atmospheric Model Intercomparison Project (AMIP) which was initiated in 1989 under the auspices of the World Climate Research Program (WCRP) with the aim to systematically validate, diagnose and intercompare the performance of AGCM in simulated various aspects of the climate system (Gates et al. 1992, 1999). During AMIP-I, over 30 AGCMs around the world were organized to carry out simulation of the evolution of the earth climate from 1979-88, subject to identical prescribed observed monthly sea surface temperature, sea ice, CO_2 concentration and solar constant. A large number of model output variables are archived and standardized and made available to the scientific community. Thanks to AMIP climate model users have gained a better appreciation of what are the strengths and weaknesses of climate model. More important, AMIP allows modelers to learn more about their own model from having independent examination of their own model outputs in comparison with other models. It is the driving force behind many efforts in model improvement in research institutions. Moreover, AMIP results have shown that even if individual model does not perform well, the ensemble means of all models can do a better job than individual models in simulating the evolution of climate. This is because model errors tend to cancel out in large model ensemble, so that the signal–to-noise ratio can be increased. The use of super-ensemble techniques (Krishnamurti et al 2000), whereby statistical weights are assigned to each model variables, at each grid point, hold promise for more reliable simulations, and climate projections on regional scales. Following on the success of AMIP-I, an expanded AMIP-II is now underway to include a wider range of variability, to accelerate model physics improvement and to improve the infrastructure for model diagnostics, validation and experimentation. At present there have been various model intercomparion projects (MIPs), tailored to various modeling communities have emerged in recent years. This included Coupled Model Intercomparison Project (CMIP) , the Seasonal Model Intercomparion Project (SMIP), Project of Intercomparison of Land Parameterization Schemes (PILPS), the Paleoclimate Model Intercomparison Project (PMIP), and many others.

3. Modeling the Asian Monsoon Climate

The Asian monsoon (AM), encompasses the vast regions spanning the Indian subcontinent, Southeast Asia and East Asia, surrounded by the Indian Ocean and the western Pacific Ocean. It is home to more than half of the world's population. The socio-economic infrastructure of the mostly agrarian societies in the AM region has been built, in large part, on the basis of a highly reproducible annual cycle of rainfall. Agriculture, drinking water, health, energy generation, and more generally the livelihood and well being of this vast human population all depend on monsoon rains. Imbedded in the large-scale monsoon circulation are powerful rain-producing weather systems, known as monsoon depressions. An anomaly of the AM in the form of a slight shifting of the monsoon rain system will cause major flooding in one place and drought in another. Droughts and floods are the major cause extensive destruction of the ecosystem, property damage, collapse of regional economies and loss of human life in the AM region.

While drought can cause long-term crippling effects on a country or a region, a single season of flooding can be devastating. For example, the wide spread monsoon flood over central and East Asia during the summer of 1998 was responsible for the loss of over 3000 human lives, damaged more than 30 million acres of farmland, and ruined over 11 million acres of crops. In all, the flooding inflicted an economic loss totaling over $12 billion US dollars to China, and brought the country's economy to its knees. Since much of world's productivity rely on the natural, economic an human resources residing within the thriving economies of the AM region, our ability to predict the interannual changes in monsoon circulation and rainfall is a critical requirement for the sustainable development of not only of the AM region, but of the world.

Understanding, modeling and predicting monsoons is also of great importance to the projections of future climate change due to the increase in the concentration of the greenhouse gases. The AAM region is one of a few places in the world for which nearly all climate models predict increased rainfall in association with global warming. Furthermore, it has been observed that the SST warming trend during the past 20 years has been the largest in the tropical oceans, especially in the Indian Ocean. Increased convection in the Indo-Pacific region associated with the warming of the Indian Ocean may be linked to long-term climate change in the North Atlantic (Hoerling et al. 2001 a,

b). Therefore an understanding of the possible effects of a warmer Indian Ocean on the AM is essential to understand the regional and global effects that may stem from global warming.

There is a large body of observational and modeling research that suggest strong interaction between the El Nino Southern Oscillation (ENSO) and the AM. The ENSO and AM cycles mutually affect each other. While neither ENSO nor the monsoon own their origin and existence to the other, there is clear evidence that their variations are affected by interactions between them (Kirtman and Shukla 2000; Lau and Wu 2001). Most intriguing is the recent observation of a dramatic drop in the relationship between Indian monsoon rainfall and ENSO in the last two decades. It has been hypothesized that the drop in the correlation between Indian monsoon rainfall and ENSO may be related to a shift of the Walker circulation, or temperature changes over Eurasia due to global warming, or the interaction of the monsoon with North Atlantic oscillations (Kumar et al. 1999; Chang et al 2001). Appropriately designed modeling experiments will shed light on the possible dynamical mechanism underlying these observations, and hypotheses.

3.1 Modeling the mean climate

The prediction of monsoon rainfall using dynamical models has been a major challenge for the climate research community in general, and the climate modeling community in particular. While it has been generally recognized that the mean monsoon system is highly stable and predictable (in the sense of a highly reproducible annual cycle), state-of-the-art climate models have been singularly unsuccessful in predicting the fluctuations about the mean annual cycle.

<Insert Table 2>

Because of the complex physical processes involved, interannual variability of the AM is generally only poorly simulated by climate models (Gadgil and Sajani 1998, Sperber and Palmer 1996). In the following, we discuss results of the WCRP/CLIVAR Monsoon Model Inter-comparison Project (MMIP). In MMIP, 10 international modeling groups collaborated in carrying out ensemble integrations for a two-year period to assess the ability of climate models to simulate the impacts of the 1997-98 El Nino on AM

anomalies (Kang et al. 2002). See Table 2 for a brief description of the individul model characteristics. Each model ensemble consists of 10 members, and each member is subject to the same lower boundary forcings from SST and sea-ice, but with different initial conditions. While the ensemble mean rainfall distribution is broadly similar to the observed (Fig. 5a and b), the difference between the model mean and the observed is quite large over the AM region, as well as the eastern equatorial Pacific and central America. Compared to the observations, the model mean tends to overestimate the rainfall over the land and underestimate over the adjacent oceanic regions. In addition, the model random noise, as measured by the deviations from the model mean is also largest in the AAM regions. In some AAM regions, the model mean bias (Fig.5c) and the random errors (Fig. 5d) are as large as, or larger than the mean rainfall (Fig. 5b). The MMIP results show that modeling the mean climate and its annual variation correctly is a prerequisite for improving simulations and predictions of climate variability and global change.

<Insert Fig. 5>

3.2 Pattern correlations

The performance of models can be evaluated against the similarity of the model rainfall patterns to the observed by the pattern correlation (P_{rms}) and the root-mean-square ratio (R_{rms}) defined by: .

$$P_{cor} = \frac{\sum_{\mathbf{r}} (X_{\mathbf{r}} - \overline{X_{\mathbf{r}}})(O_{\mathbf{r}} - \overline{O_{\mathbf{r}}})}{\sigma_X \sigma_O}, \quad R_{rms} = \frac{\sigma_X}{\sigma_O}$$

where X is a model variable, and O is the corresponding observation. The summation is over the spatial coordinate **r**, over the chosen domain, the overbar represents the spatial average, and s is the spatial standard deviation. P_{rms} and R_{rms} have been computed for each ensemble member, for each model and for different seasons. The closer P_{rms} and R_{rms} to unity, the better is the model performance.

Fig. 6a and 6b show the model ensemble mean values of P_{rms} and R_{rms} for each model as bar charts, for. December-January-February (DJF) and June-July-August (JJA)

for two years, over the Indo-Pacific region 30° S-30° N, 60° E-90° W). The standard deviation of P_{rm} and R_{rms} for each model and for each season is indicated by the vertical lines inside the bars. The all-model ensemble mean is show in the far right column. From Fig. 6. The performance of individual models can be compared with the others and to the all-model ensemble mean. It can be seen that the mean P_{rms} for individual model ranges from 0.2 to 0.8 (Fig.6a). The correlations seem to be higher during the boreal winter compared to the boreal summer, indicating that the models tend to capture the physics of the wintertime rainfall and circulation regimes better than that for the summer. All models seem to have a higher correlation for DJF 1998, when the El Nino signal is at a peak, suggesting that all models are responsive to the warm phase of the El Nino. If the eastern portion of the domain (east of the dateline) is excluded in the pattern correlation calculation, P_{rms} reduce dramatically (not shown), indicating that most of the good correlation is contributed by the rainfall directly responding to the El Nino SST over the central and eastern Pacific. The ensemble mean P_{rms} for each model tends to be higher than most individual ensemble member. Similarly, P_{rms} for the model mean (columns to the extreme right) are generally among the top tier of the better performing models. The picture is quite similar for R_{rms}. (Fig.6b). Here, about half of the models have R_{rms} greater than 1.0, and about half less than 1.0. The rms ratio for the individual member (whose range is indicated by the vertical line) tend to be larger than the model mean. This is because the model mean tends to smooth out the spatial features. The all-model R_{rms} is less than one, suggesting the models collectively underestimate the observed variability of the rainfall anomalies in the Indo-Pacific region. This is expected, because the all-model mean is derived from a large number (in this case, for 10 models and 10 member per ensemble, 10x10 =100) of model realizations, while the observation is just a one-time realization of the real system. In all, the multi-model ensemble mean provides simulation with more reliability and skill comparable to the top performing models. Other more sophisticated ensemble means, such as the super-ensemble procedure, can produce simulations with skills that exceed all the individual models (Krishnmurti et al 2000).

<Insert Fig.6>

Another important finding of MMIP, is that models which can simulate a realistic climatology, generally have better skill in simulating interannual variability. Fig. 7a shows scatter plots of the climatological pattern correlation vs. the anomaly pattern correlation of rainfall of the models with respect to observations over the Indo-Pacific region. Fig.7b show the same, but for R_{rms}. The climatological quantity is a measure of how good the models are in simulating the annual cycle, and the anomaly, how good the model simulate interannual variability. Prediction skills are based on the ability of the models to simulate the interannual anomalies above and beyond those provided by the climatology. The positive slope of the regression lines in Fig.7a and 7b suggest that a good simulation of climatology generally imply a good simulation of the interannual anomaly. A model that has a good climatology is an indication that the physical and dynamical processes are well represented, and therefore provides some assurance that the model may be used for anomaly climate predictions on interannual or longer time scales.

<Insert Fig. 7>

3.3 *Response to 1997-98 ENSO*

Intercomparison of the simulations of the impact of the 1997-98 El Nino indicates that AGCMs generally simulate reasonably well the eastward shift of the Walker circulation (see discussion in Section 2.3) associated with the anomalous warm SST of the central and eastern Pacific (Ju and Slingo 1995, Lau and Nath 2000). Figure 8 shows a comparison of the observed and the simulated model mean velocity potential difference (JJA 1997 minus JJA 1998) at 200 mb. Here, the positive contours indicate anomalous large scale ascent over the central and eastern Pacific, and the negative contours anomalous descent over the Indian Ocean. However, the difference map between the model mean and observation (Fig. 8c), indicates that large errors are found in the Asian monsoon region, with the model over-estimating the anomalous sinking motion over the maritime continent and the rising motion over the South China and East China Seas. This may be interpreted as the AGCM's inability to model the regional anomalous induced by the Walker circulation (Soman and Slingo 1997, Lau and Wu 2001). The models tend to

disagree most among themselves over the Indian Ocean and the tropical western Pacific (Fig. 8d).

<Insert Fig. 8 >

Many modeling studies have been conducted to unravel the causes of the record summer monsoon flooding over central East Asia (Shen et al. 2001, Wang et al 2000). Fig. 9 shows the ensemble mean of the rainfall and 850 mb wind anomalies (1998 minus 1997) for JJA and for each model participating in the CLIVAR MMIP. For comparison, the observation is shown in the bottom right panel labeled CMAP. The observation shows a zonally oriented rainfall anomaly pattern with reduced rainfall over the tropical western Pacific, and Indo-China along 10°N, increased rainfall over the maritime continent /equatorial eastern Indian Ocean, and the subtropics between 30 – 40°N. The regions with rainfall increase are located on the northern and southern flank of a subtropical anticyclone, which is very pronounced during JJA 1998. The former is related to the *Mei-yu* rainbelt of East Asia and the latter to the development of the Intertropical Convergence Zone (ITCZ) over the eastern Indian Ocean and the MC. Both features were enhanced during JJA 1998. Anomalous low-level westerlies found along 10° N from the central/western Pacific across Indo-China to the Bay of Bengal and India. Near Japan and the northwestern Pacific, the large-scale circulation shows wave-like features, associated with fluctuation of the subtropical jetstream (Lau and Weng 2002). During JJA 1997, the Walker Circulation shifts eastward in respond to the El Nino SST forcing, inducing strong downward motion over the maritime continent and suppressing the ITCZ. The anomalous anticyclone is the cause of the major flooding over the Yangtze River Valley during JJA 1998 (Lau and Wu 2001, Lau and Weng 2001, Shen et al 2001). The establishment of the anticyclone is related to descending motion associated with the eastward shift of the Walker circulation, and also to amplification by local air-sea interaction.

<Insert Fig. 9>

The model ability to simulate the aforementioned features are generally not very impressive. While most models show the correct sign of the large-scale response in the AM region, most models, except perhaps SNU, fail to simulate the observed zonally oriented rainfall structure. It is clear from the results shown that the simulation of the East Asian monsoon rainfall anomalies are critically dependent on the anomalous anticyclone, which governs the moisture available for precipitation. Because the anticyclone is generated by large-scale dynamics, its broad feature is represented in most models. However, it is the simulation of the exact location and magnitude of the anticyclone that is required in order for climate models to simulate the regional AM rainfall anomalies, and hence the severe floods and droughts in the AM region. The use of higher resolution climate models, or the use of downscaling methodologies is required.

The performance of AGCMs to simulate the 1997-98 rainfall anomalies can also be evaluated from examination of the distribution of model climate states represented as two dimensional scatter plots along axes representing key climate variables. Shown in Fig. 10 are model rainfall anomalies averaged over selected domains (labeled by latitude-longitude boundaries in Fig. 10), plotted against the Southern Oscillation Index (SOI). The domains are for the AM region as a whole, and for its components parts over the maritime continent (MC), the South Asian Monsoon (SAM) and the South East Asian Monsoon (SEAM). Each data point represents one ensemble member of each model. The heavy shaded symbols represent the observed states. It can be seen that the models are quite responsive to the El Nino signal, in that there is a clear separation of model states between 1997 and 1998 along the SOI axis in all panels. Indeed, the models tend to overestimate the east-west seesaw, as evident in the larger spread along the SOI axis compared to the observations. For the AM region as a whole (Fig.10a), a reduction in rainfall during 1997 compared to 1998 can be discerned. This reduction is mainly contributed by the rainfall anomalies over MC, which is situated at the descending branch of the Walker circulation. For the SAM and SEAM region, the large clusters of model states for 1997 and 1998, and the lack of obvious shift of the center of gravity of the clouds in the y-axis during these two years suggests that there are large rainfall variability, but they have no significant climate impact from the El Nino in these two monsoon subregions, in agreement with observations. The observed AM anomalies

represents only a single realization drawn from an intrinsic distribution effected by SST forcings identical to the 1997-98 El Nino. To the extent that the model can mimic the real climate, the cluster of model climate states around the observation provides a measure of that intrinsic distribution. AMIP results suggest that models that simulate well the seasonal cycle is a prerequisite for better simulation of the interannual variability of AM rainfall.

<Insert Fig. 10>

3.4 Intraseasonal variability

One of the key characteristics of the AM is the presence of a rich spectrum of subseasonal scale variability, generally referred to as intraseasonal variability. These include quasi-periodic oscillations from 30-60 days, 10-20 days and transient waves of 3-5 days. The intraseasonal variability are generated by internal atmospheric dynamics but strongly modified by sea surface temperature and land surface processes. They are responsible for the modulation of monsoon onsets, breaks and evolution regionally. Intraseasonal variability, especially those in the lower frequency end of the spectrum, can have strong impacts on the seasonal mean monsoon climate. Over different regions, they can either strengthen or weaken the direct influence by ENSO on the AM. It has been suggested that, the near normal monsoon rainfall over India during the strong El Niño of 1997-98 may be due to the effects of pronounced intraseasonal variability, which brought copious rainfall to many parts of India, in spite of the tendency of ENSO to weaken the AAM (see discussion in previous section).

Modeling intraseasonal variability of the AM is a very challenging problem. Models generally fail to capture the phase locking between intraseasonal variability and the seasonal cycle. For example, at the longitude of the Bay of Bengal (Fig. 11), the ensemble mean of MMIP models depicts an over-simplified picture of the monsoon evolution with a sudden onset of the South Asia monsoon near the middle of May and beginning of June. However the models fail to reproduce the complex intraseasonal structure associated with the evolution of the monsoon rain-belt as observed. During JJA, the models show a much more quiescent atmosphere over the oceanic regions near the equator compared to the observed. Similarly, at 130° E, the models seem to capture

the broad seasonal evolution, but they fail to capture the climatological intraseasonal variability during JJA which is very prominent in the observation. In particular, the models fail to reproduce the development of the monsoon rainbelt associated with the *Mei-yu* front from 20° N to 40° N. The *Mei-yu* front is the major climate features that dominate the climate of continental East Asia, Korea and Japan (Lau and Li 1984). The absence of such features in the coarse resolution climate models is an endemic problem in almost all AGCMs (Lau et al 1996, Liang et al 2001) in indicate that downscaling approaches may be needed to capture this unique feature of the East Asian monsoon.

<Insert Fig. 11>

3.5 Land-atmosphere feedback

Recent modeling studies have shown that land-atmosphere processes can affect monsoon and monsoon-ENSO relationship by altering the energy and water cycles within the AM regions, through surface heat fluxes and hydrologic feedback mechanisms. Lau and Bua (1998) carried out a series of numerical experiments using a NASA global climate model, similar to those described in Section 2.3. Their results suggest an atmosphere-ocean-land feedback scenario as illustrated in Fig.12. If the soil moisture content of the Asiatic land mass is abnormally high during the start of a monsoon season, land surface evaporation will be increased. This will lead to increased moistening of the atmospheric boundary layer, more unstable air masses and hence more convection and rainfall, resulting in a positive feedback leading to further moistening of the land region. However, the cloudy sky condition stemming from enhanced convection will shield off and reduce solar radiation from reaching the land surface, causing the land to cool. As the land mass cools off, the resulting decreased land-sea thermal contrast can only support a weaker large-scale monsoon circulation, with reduced monsoon rainfall, thus producing a negative feedback, which halts further increase in soil moisture. These feedback mechanisms are dependent not only on local processes but also on the remote forcing such as forced large scale descent or ascent over the AM region by ENSO. The large-scale vertical motions provide a strong control on atmospheric stability and initiation of convection. Even though the ENSO remote forcing has relatively slow time

scales, its impact may be sufficient to tip the delicate balance of the aforementioned local feedback processes causing either the amplification of a given climate state or transition from one state to the other. The hypothesis needs to be verified with additional data, analyses and further experimentations with other climate models with detailed land surface processes.

<Insert Fig. 12>

In summary, studies up to now have shown that a large portion of the predictable part of interannual variability of the monsoon rainfall is forced by the slowly varying boundary conditions at the earth's surface. However, no climate model has been able to replicate even the simplest empirical relationship between the SST anomalies and monsoon rainfall anomalies. It is unclear at this stage whether the inability of current models to simulate and predict monsoon rainfall is due to model deficiencies or due to intrinsic lack of predictability of the monsoon. It is likely that both play important roles.

5. Future Challenges

In this Chapter, we have discussed the importance of modeling in providing better understanding of causes of regional climate anomalies, and in predicting future climate evolution, using the AM climate as a specific example. Given that models will be increasingly used for climate predictions of all time scales, it is important to keep in mind that large uncertainties exists and that not all aspects of model predictions have the same degree of reliability. The challenge is to how to reduce these model uncertainties, and to make climate forecast more reliable and useful. The following are suggested steps that should be taken to move in that direction. Because each of the steps involve complex procedures and organized efforts, successfully implement these steps will take years of sustained efforts by the science community.

- *Use finer spatial and temporal resolution.* As stated previously, one of major uncertainties in climate models stems from the lack of spatial and temporal resolution, as a result regional to sub-regional scale features are not well

represented. Yet it is these sub-regional features and short-term events that are causes the most socio-economic damages. With the advances in computational power, it is now possible to run climate models with high resolution globally for extended periods. For example the European Center for Medium Range Forecasting is running its operational model for medium and long-range weather predictions of the order of 50 km resolution, and the Frontier Climate Change Research Program of Japan is running the Earth Simulator at 10-20 km resolutions. One of the most obvious improvements in going to higher resolution is the better simulation of orographic rain, especially in regions of complex topography. Even with the increased resolution, for some applications such as catchment scale water resource management, resolution of less than a few kilometers may be required. In this respect, the downscaling techniques using regional climate models and macroscale hydrology models will be important.

- *Improve model physics.* While increasing resolution will reduced model uncertainty and improve the geophysical fluid dynamic aspects of climate models, the major culprit of model uncertainty still lie in the inadequacy of representation of physical processes, which determine the forcing functions of the model. If a model is driven by erroneous forcing functions, no matter how good the flow fields can be simulated, it will not give the right answers. Improvement of physical representation in models is therefore paramount and should be focused on processes which are key drivers of the earth's hydrologic cycles. These include cumulus heating in the tropics, aerosol-cloud-radiative processes, fluxes at the air-sea and air-land interfaces, land surface and vegetation processes. Improving model physics is an extremely difficult and tedious endeavor, because the physics of climate is very complex and inter-woven. Improving a physical process in a stand-alone model, does not necessarily mean that it will give better performance in a coupled model. Likewise, improving one part of the system does not always lead to improvement of other parts. Hence the process of improving model physics can

be very difficult and tedious, calling for multiple tests and validation with observations under a variety of conditions. Substantial improvements are not likely to come in the short-term, but sustained organized efforts by the scientific community are required. In some sense, we have exhausted much of the reliable information that can be derived from current climate models. Unless model physic improvement is taken seriously, model uncertainties will remain unacceptably large.

- *Improve data for model validation* One of the major stumbling block for model improvement is the lack of detailed data suitable for model validation and improvement. Given the vast amount of data obtained from ground-base and satellite atmospheric and oceanic observations, field campaigns and special measurement platform, it may seem a bit puzzling that there is still a shortage of data for model validation. The reason is that for model physics improvement very specialized data with high spatial and temporal resolutions, directly relevant to the model parameters, are required. These data are often not direct observables in the climate system, but derived quantities from the observables and therefore have large uncertainties themselves. Often, they required special intensive observation platforms, which for practical purpose can only be carried out over a short period in field campaigns. To be sure, besides new data from future field campaigns, there are data that can be extracted from the vast satellite and operational historical data base, as well as various enhanced observational sites to be used for model validation and physics improvement. There is a need for coordinating and extracting global, regional and site data from various sources, and making them available for model improvement and prediction.

- *Model prediction applications* Climate forecasts both short and long-term have tremendous potential benefits for society. Accurate seasonal forecasts of winter storm, summer drought and flood, hurricane frequencies will result in substantial savings and in reduction of damaged properties and loss of human

life. Skilful prediction of El Nino using coupled ocean-atmosphere models have resulted in limiting its adverse impacts on food production and fisheries by advanced planning, and implementation of mitigating measures in many regions around the world. To realize the full benefit of climate forecasts, climate models should be coupled with cost and risk models for agriculture, food production, water resource management and other societal applications, to reduce vulnerabilities to natural hazards and climate change.

Acknowledgment

This work is supported by the Global and Modeling and Diagnostic Analysis Program of the NASA Earth Science Office.

References

Bengtsson L. and A. J. Simmons, 1983: Medium range weather prediction – operational experience at ECMWF. *Large-Scale Dynamical Processes in the Atmosphere.* . B. J. Hoskins and R. P. Pearce, Academic Press, pp. 337-63.

Charney J. G., Fjortoft , R., von Neumann J., 1950: Numerical integration of the barotropic vorticity equation. *Tellus* **2**, 237-254.

Chang, C. P., P. Harr, and J. Ju, 2001: Possible role of Atlantic circulations on the weakening Indian monsoon rainfall-ENSO relationship. *J. Climate.*, **14**, 2376-2380.

Fox-Rabinovitz M.S, Takacs L.L, Govindaraju R.C., et al. 2001: A variable-resolution stretched-grid general circulation model: Regional climate simulation. *Mon. Wea. Rev.* **129**, 453-469

Gadgil, S., S. Sajani, 1998: Monsoon precipitation in the AMIP runs. *Climate Dynamics*, **14**, 659-689.

Gates, W. L. and collaborators, 1999: An overview of the results of the Atmospheric Model Intercomparison Project (AMIP-I). *Bull. Am. Meteor. Soc.*, **80**, 29-55.

Gates, W. L., 1992: AMIP: The atmospheric model intercomparison project. Bull. Amer. Meteoro. Soc., 73, 1962-1970.

Georgi, P, L. O., Mearns, 1991: Approaches to simulations of regional climate change: a review. *Rev. Geophys* **29**: 191-216.

Gilchrist A., 1977: An experiment in extended rang prediction using a general circulation model and including the influence of sea surface temperature anomalies. *Beitr. Phys. Atmos.*, **50**, 25-40.

Gilchrist, A., 1981: Simulation of the Asian summer monsoon by an 11-layer general circulation model. In Monsoon Dynamics, Eds. M. J. Lighthill & R. P Pearce, Cambridge University Press. Pp. 131-145

Hewitson, B. C., and R. G. Crane, 1996: Climate downscaling: techniques and application. *Clim. Res.*, **7**, 85-96.

Hoerling et al. 2001: The midlatitude warming during 1998-2000. *Geophys. Res. Letters*, **28**, 755-758.

Hoerling, M. P., J. W. Hurrell, and T. Xu, 2001: Tropical origin for recent North Atlantic Climate Change, *Science*, **292**, 90-92.

Hoffman, R. N., and E. Kalnay, 1983: Lagged average forecasting, an alternative to Monte Carlo forecasting. *Tellus*, **35a**, 100-118.

Ju, J. and J. Slingo, 1995: The Asian summer monsoon and ENSO. *Quart. J .Roy Meteor. Soc.*, **121**, 1133-1168.

Kalnay, E., M. Kanamitsu, R. Kistler, W. Collins, D. Deaven, L. Gandin, M. Iredell, S. Saha, G. White, J. Woollen, Y. Zhu, M. Chelliah, W. Ebisuzaki, W. Higgins, J. Janowiak, K. C. Mo, C. Ropelewski, J. Wang, A. Leetmaa, R. Reynolds, R. Jenne and D. Joseph, 1996: The NCEP/NCAR 40-year reanalysis Project. *Bull. Am. Meteor. Soc.*, **77**, 437-471.

Kang, I. S., K. Jin, B. Wang and K. M. Lau, 2001: Intercomparison of the climatological variations of the Asian summer monsoon rainfall simulated by 10 GCMs. *Climate Dynamics* (accepted).

Kang, I.-S., K. Jin, K. M. Lau, J. Shukla, V. Krishnamurthy, S. Schubert, D. Waliser, W. Stern, V. Satyan, A. Kitoh, G. Meehl, M. Kanamitsu, V. Ya Galin, J. K. Kim , G. Wu and Y. Liu, 2001 Intercomparison of GCM simulated anomalies associated with the 1997-98 El Nino. *Bull. Amer. Meteor. Soc.* **(accepted)**

Kawamura, R., M. Sugi, T. Kayahara and N. Sato, 1998: Recent extraordinary cool and hot summers in East Asia simulated by an ensemble climate experiment. *J. Meteor. Soc. Japan,* **76**, 597-617.

Kirtman B. P. J. Shukla, 2000: Influence of the Asian summer monsoon on ENSO. *Quart. J. Roy. Meteor. Soc.,* **126**, 213-239.

Koster, R., Randal, D., M. J. Suarez, and M. Heiser, 2000: Variance and predictability of Precipitation at seasonal-to-interannual timescales. *J. Hydromet.* **1**, 26-46.

Krishnamurti T.N., C. M., Kishtawal, D. W., Shin , C. E., Williford, 2000: Improving tropical precipitation forecasts from a multi-analysis superensemble. *J. Climate*, **13**, 4217-4227.

Kumar, K. Krishna, Balaji Rajagopalan, Mark A. Cane, 1999: On the weakening relationship between the Indian Monsoon and ENSO. *Science*, **284**, 2156-2159.

Lattenmaier, D. P., A. W. Wood, Palmer, R. N., E F. Wood, E. Z., Stakhiv, 1999: water resources implications of global warming: A US regional perspective. *Climate Change*, **43**, 537-579.

Lau, K.M. and H. Weng, 2002: Recurrent teleconnnection patterns linking summertime precipitation variability over East Asia and North America. *J. Meteor. Soc.. Japan* (accepted).

Lau, K. M. and H. T. Wu, 2001: Intrinsic modes of coupled rainfall/SST variability for the Asian summer monsoon: a re-assessment of monsoon-ENSO relationship. *J. Climate*, **14**, 2880-2895.

Lau, K. M. and H. Weng, 2001: Coherent modes of global SST and summer rainfall over China: an assessment of the regional impacts of the 1997-98 El Nino. *J. Climate* , **14**, 1294-1308.

Lau, K-M., and W. Bua, 1998: Mechanism of monsoon-Southern Oscillation coupling: insights from GCM experiments. *Climate Dynamics,* **14**, 759-779.

Lau, K.-M., J. H. Kim and Y. Sud, 1996: Intecomparison of hydrologic processes in AMIP GCMs. *Bull. Am. Met. Soc.*, **77**, 2209-2227.

Lau, N. C., and M. J. Nath, 2000: Impact of ENSO on the variability of the Asian-Australian monsoons as simulated in GCM experiments. *J. Climate*, **13**, 4287-4309.

Liang, X., W. C. Wang and A. N. Samel, 2001: Biases in AMIP model simulations of the east China monsoon system. *Climate Dynamics*, 17 291-304.

Manabe S. and R. T. Wetherald 1975, The effects of doubling the CO2 concentration on the climate of a general circulation model. *J. Atmos. Sci.*, **32**, 3-15.

Manabe S., K. Bryan and M. J. Spelman 1979: A global ocean-atmosphere climate model with seasonal variation for future studies of climate sensitivity. Dyn. Atmos. Oceans, 3. 393-426.

Palmer, T. N., 1993: Extended range atmospheric predictin and the Lorenz model. *Bull. Amer. Meteor. Soc.*, **74**, 49-66.

Shen, X., M., Kimot., A., Sumi, A., Numagauti, A., and J., Matsumoto, 2001: Simulation of the 1998 East Asian summer monsoon by the CCSR/NIEW AGCM. *J. Meteor. Soc., Japan* **79**, 741-757.

Shukla, J., J. Anderson, D. Baumhefner, C. Brankovic, Y. Chang, E. Kalnay, L. Marx, T. Palmer, D. Paolino, J. Ploshay, S. Schubert, D. Strass, M. Suarez and J. Tribbia, 2000: Dynamical seasonal prediction. *Bull. Am. Meteor. Soc.*, **81**, 1593-2606.

Simmons A. J., and L. Bengtsson, 1998: Atmospheric general circulation models: their design and use for climate studies. In Physical-based modeling and simulation of climate and climate change. Ed. M. E. Schlesinger, Part I: Kluwer Academic Publishers, 624pp.

Smagorinsky, J., Manabe S., Holloway J. L., 1965: Results from a nine-level general circulation model of the atmosphere. *Mon. Wea. Rev.*, **93**, 727-768.

Soman, J. K., and J. Slingo, 1997: Sensitivity of Asian summer monsoon to aspects of sea surface temperature anomalies in the tropical Pacific Ocean. *Quart. J. Roy. Meteor. Soc.*, **123**, 309-336.

Sperber K. R., Palmer, T. N., 1996: Interannual tropical rainfall variability in general circulation model simulations associated with the atmospheric model intercomparison project. . *J. Climate* , **9**, 2727-2750.

Sperber, K. R., S. Hameed, G. L. Potter and J. S. Boyle, 1994: Simulation of the northern summer monsoon in the ECMWF model: Sensitivity to horizontal resolution. *Mon. Wea. Rev.* 122, 2461-2481.

Stefanova L., Krishnamurti T. N., 2002: Interpretation of seasonal climate forecast usig Brier skill score, the Florida State University superensmeble and the AMIP-I data set. J. *Climate,* **15**, 537-544.

Tracton, M., S. Kalnay and E. Kalnay, 1993: Operational ensemble predction at the National Meteorological Center: Practical aspects. *Wea. Forecasting*, **8**, 379-398.

Von Storch H. and F. W. Zwiers, 1999: Statistical Analysis in Climate Research. Cambridge University Press. pp 484.

Wang, H..-J., T. Matsuno T., and Y. Kurihara, 2000: Ensemble hindcast experiments for the flood period over China in 1998 by use of the CCSR/NIES AGCM. *J. Meteor. Soc. Japan*, **78**, 357-365.

Table 1 Possible experimental designs for climate sensitivity experiments. The letters C and O denotes climatology and observation respectively. A check mark indicates an interactive component

	Atmosphere	Ocean	Land
Exp-I (control)	√	C	√
Exp-II	√	O	√
Exp-III	√	O	C
Exp -IV	√	C	C
Exp -V	√	√	√

Table 2 Description of the atmospheric GCMs participating in the CLIVAR/Asian-Australian Monsoon GCM intercomparison project

Group	Institution	Model	Resolution	Radiation	Convection	Land Surface Process	Cloud Formulation
COLA	Center for Ocean-Land-Atmosphere Studies (U.S.A.)	COLA 1.11	R40L18	Lacis and Hansen (74) Harshvardhan *et al.* (87)	Relaxed Arakawa-Schubert (Moorthi and Suarez 92)	Sib model, Xue *et al.* (91)	Hou (90) based on Slingo (87)
DNM	Institute of Numerical Mathematics (Russia)	A5421	4°_5°, L21	Slingo (89) Chou *et al.* (93)	Betts (86)	Volodin and Lykossov (98)	Slingo (87)
GEOS	NASA/GSFC (U.S.A.)	GEOS-2	2°_2.5°, L43	Chou and Suarez (94)	RAS (Moorthi and Suarez 92)	Schemm *et al.* (92)	Slingo and Ritter (85)
GFDL	Geophysical Fluid Dynamics Laboratory (U.S.A.)	DERF GFDLSM V197	T42L18	Lacis and Hansen (74) Schwarzkopf and Fels (91)	RAS (Moorthi and Suarez 92)	Deardorff (78)	Slingo (87), Gordon (92)
IAP	Institute of Atmospheric Physics (China)	SAGCM 1.1	R15L9	ESFT Shi (81)	MCA (Manabe *et al.* 65), No shallow convection	Sib model, Xue *et al.* (91)	Prescribed
IITM	Indian Institute of Tropical Meteorology (India)	HadAM2b V4.0, UKMO	2.5°_3.75°, L19	Ingram (96) Slingo & Wilderspin (86)	Mass flux penetrative convection scheme (Gregory and Rowntree 90)	Smith (90a)	Smith (90b)
MRI	Meteorological Research Institute (Japan)	MRI GCM2	4°_5°, L15	Lacis and Hansen (74) Shibata and Aoki (89)	Arakawa-Schubert, Tokioka *et al.* (88)	Katayama (78), Kitoh et al. (88)	Tokioka *et al.* (84)
NCAR	National Center for Atmospheric Research (U.S.A.)	CCM3	T42L18	Kiehl *et al.*(98)	Mass flux scheme (Zhang and McFarlane 95)	Land surface model (Bonan 98),	Slingo (87), Kiehl (94)
SNU	Seoul National University (Korea)	SNU V.2	T31L20	Nakajima and Tanaka (86)	Simplified RAS, Diffusion-type shallow convection	Land surface model (Bonan 98),	Le Treut and Li (91)
SUNY	State University of New York (U.S.A.)	GLA GCM – 01.0	4°_5°, L17	Harshvardhan *et al.* (87)	Modified Arakawa-Schubert	Deardorff (78)	Sud and Walker (92)

Figure Captions

Fig. 1 Synergistic application of observations and models for climate diagnostic and prediction studies.

Fig. 2 An illustration of the model grid and basic physical processes in a climate model, consisting of the atmosphere, ocean and land. (Reproduced from McGuffie and Henderson-Sellers (2001) by permission of the International J. of Climatology).

Fig. 3 Sea-level pressure patterns showing the spatial structure of the Southern Oscillation for (a) ALO, (b) AO, (c) AL and (d) A. See text for definition of symbols. Contour interval is 1 mb (adopted from Lau and Bua 1998).

Fig.4 Downscaling global climate signals for regional and sub-regional scale applications

Fig. 5 (a) Pattern correlation coefficient between the simulated and observed precipitation anomalies for each model and each season over the Monsoon-ENSO region (30° S-30°N, 60°E–90°W). (b) Root-mean-square (rms) of the simulated precipitation anomalies over the Monsoon-ENSO region, normalized by the observed rms. The vertical line in the bar indicates the range of the correlation and rms values of individual run, and the black square represents the ensemble mean. (Adopted from Kang et al. 2000).

Fig. 6 Pattern correlation of ensemble anomalies of each model over the ENSO-Monsoon domain (y-axis) vs. that of the corresponding climatology (x-axis) for the 97-summer (open circle) and 97-98 winter (dark circle) seasons. (b) As in (a), except for the normalized rms.

Fig. 7. Spatial distribution of climatological rainfall for (a) observations from 1979-1998. (b) ensemble mean of all models, (c) Model minus Observations differences, and (d) rms deviations from all-model mean.

Fig. 8 Anomalous velocity potential (JJA 1998 minus JJA 1997) for (a) Observed, (b) all-model mean and (c) Model minus observed and (d) standard deviation from all model-mean.

Fig. 9 Scatter plots showing the distribution of anomalous precipitation vs. the Southern Oscillation Index for (a) the entire AA monsoon region, (b) the Maritime

Continent, (c) the South Asian monsoon region, and (d) the Southeast Asian monsoon region. The latitude-longitude boundary of each domain is indicated. Unit for precipitation is mm/day and for SOI is in mb.

Fig. 10 Rainfall (mm/day) and 850 mb wind (m/s) differences (JJA 1998 minus JJA 1997) for individual models participating in CLIVAR MMIP. The observation is shown in the right land bottom panel. See Table 2, for model acronyms and descriptions.

Fig. 11 Time-latitude cross section of climatological pentad-mean precipitation. (a) and (b) are for the model composite and the CMAP observations along the longitude of 90E. (c) and (d) are for longitude 130° E. (Adopted from Kang et al. 2000)

Fig. 12 Schematic showing possible land-atmosphere feedback mechanisms associated with fluctuations of the water and energy cycles, in leading to extreme floods or prolonged drought events in monsoon region. (Adopted from Lau and Bua 1998)

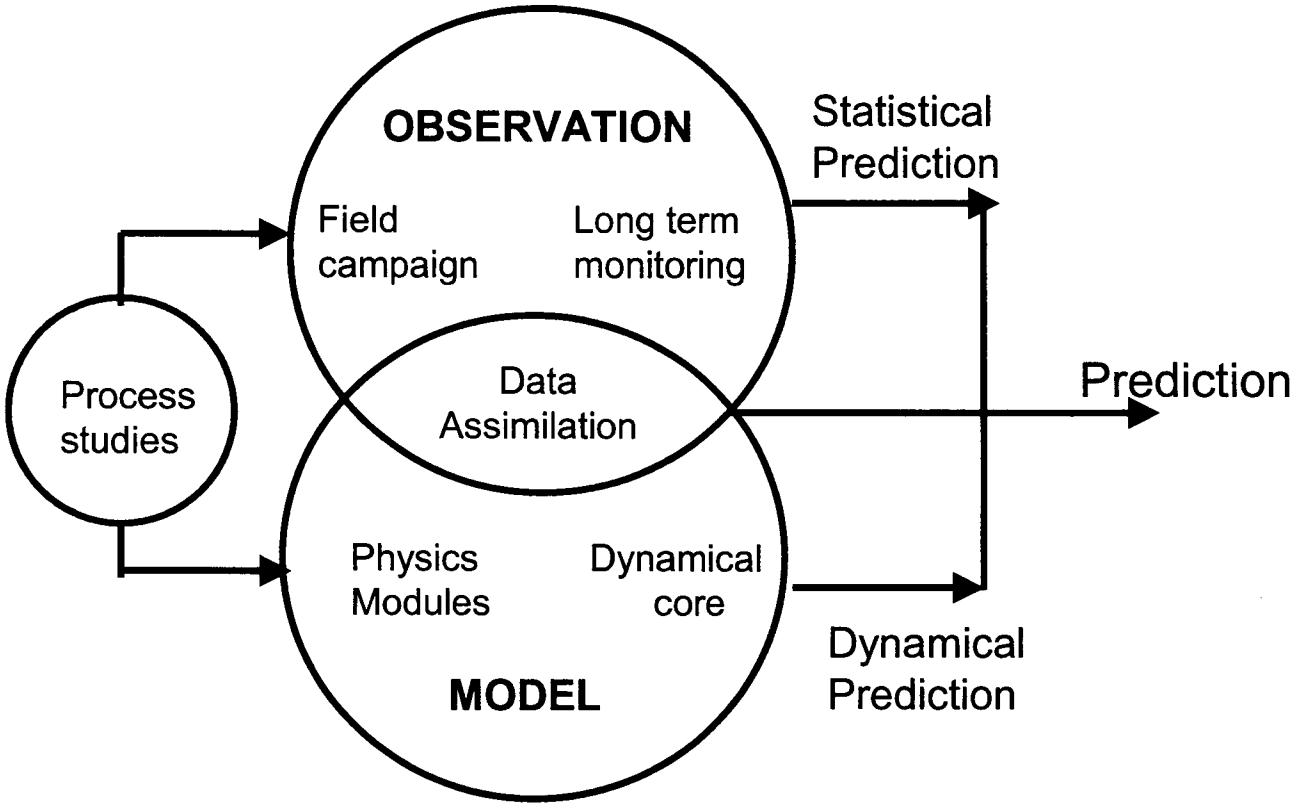
OBSERVATION
Field campaign
Long term monitoring
Statistical Prediction
Process studies
Data Assimilation
Prediction
Physics Modules
Dynamical core
MODEL
Dynamical Prediction

Fig.1

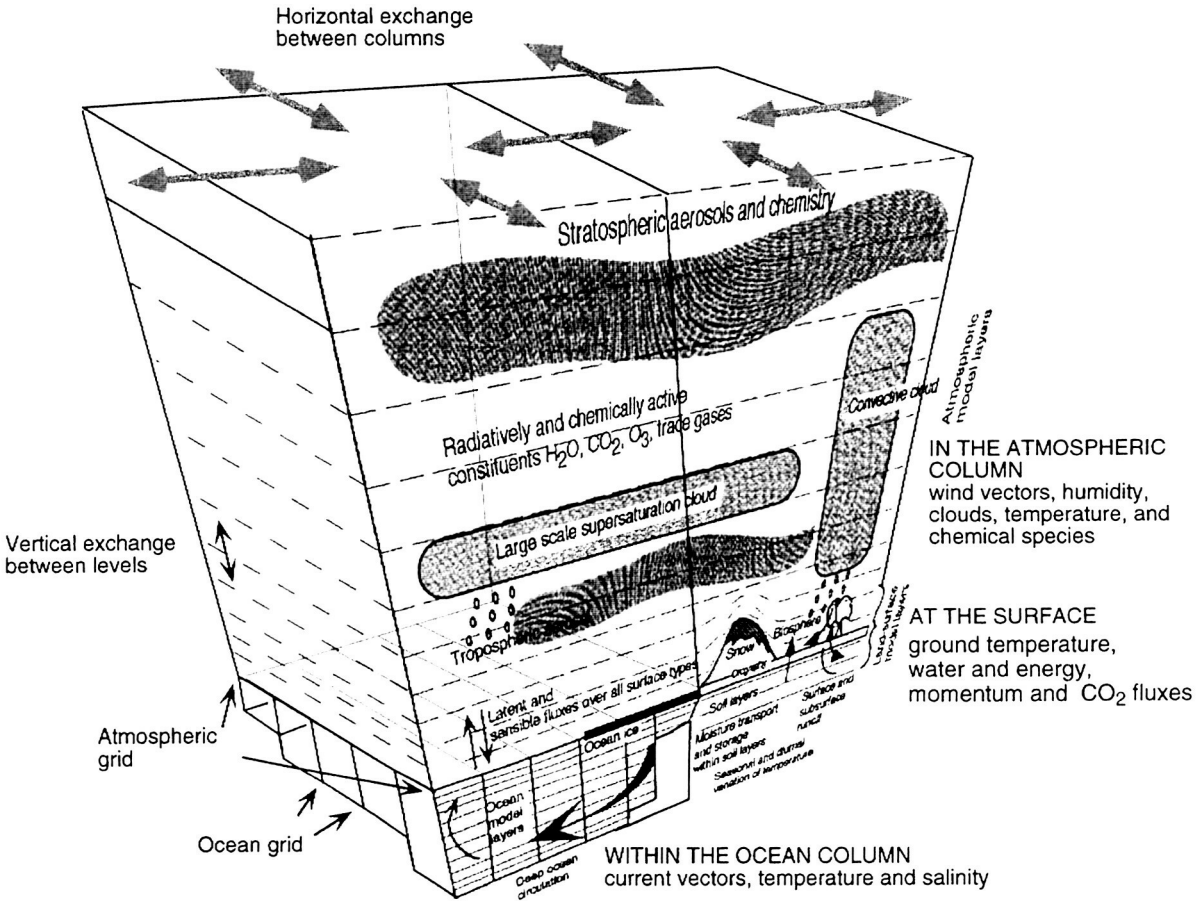
Horizontal exchange
between columns
Stratospheric aerosols and chemistry
Radiatively and chemically active
constituents H_2O, CO_2, O_3, trace gases
Convective cloud
Large scale supersaturation cloud
Troposphere
Vertical exchange
between levels
Atmospheric
grid
Ocean grid
Latent and
sensible fluxes over all surface types
Ocean ice
Snow
Biosphere
Soil layers
Moisture transport
and storage
within soil layers
Ocean
model
layers
Deep ocean
circulation
IN THE ATMOSPHERIC
COLUMN
wind vectors, humidity,
clouds, temperature, and
chemical species
AT THE SURFACE
ground temperature,
water and energy,
momentum and CO_2 fluxes
WITHIN THE OCEAN COLUMN
current vectors, temperature and salinity

Fig. 2

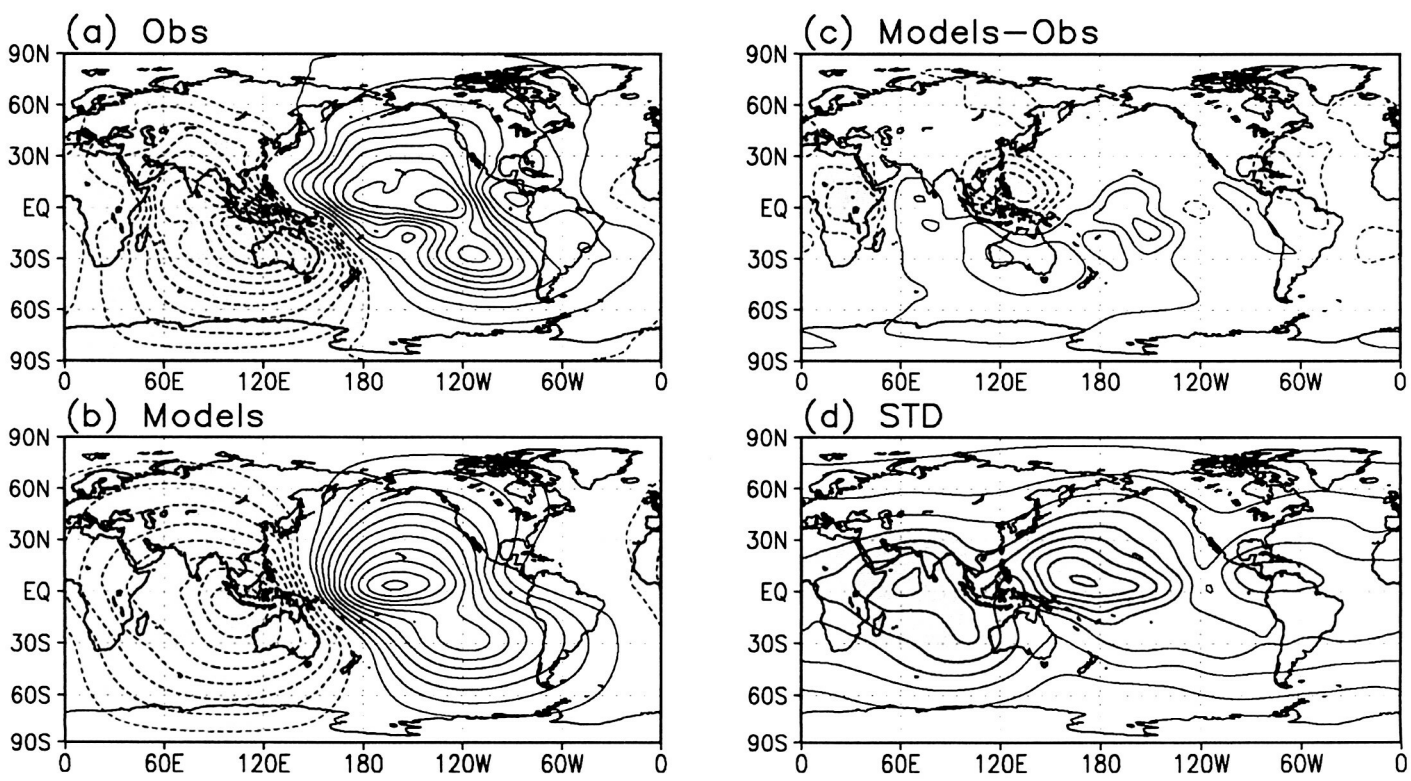
VELP(x10⁶ m²sec⁻¹). Diff (JJA1998−JJA1997)
(a) Obs
(c) Models−Obs
(b) Models
(d) STD
90N
60N
30N
EQ
30S
60S
90S
0
60E
120E
180
120W
60W
0

Fig.8

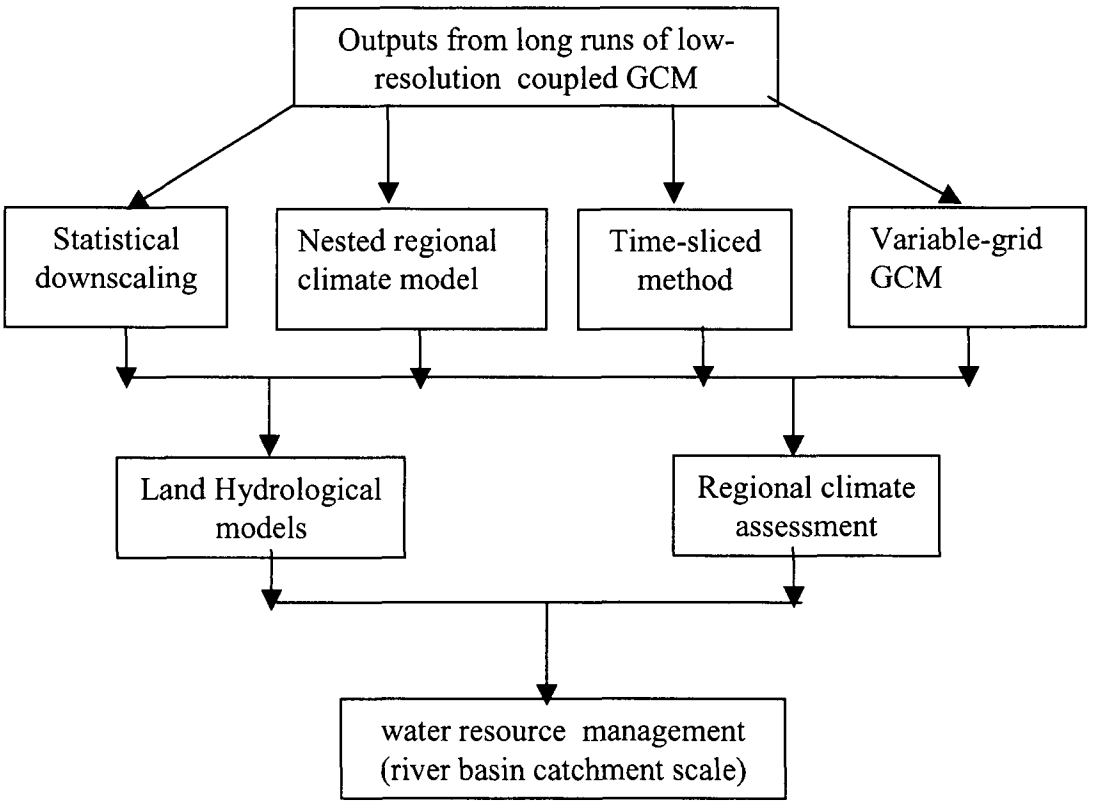
Outputs from long runs of low-resolution coupled GCM
Statistical downscaling
Nested regional climate model
Time-sliced method
Variable-grid GCM
Land Hydrological models
Regional climate assessment
water resource management (river basin catchment scale)

Fig.4

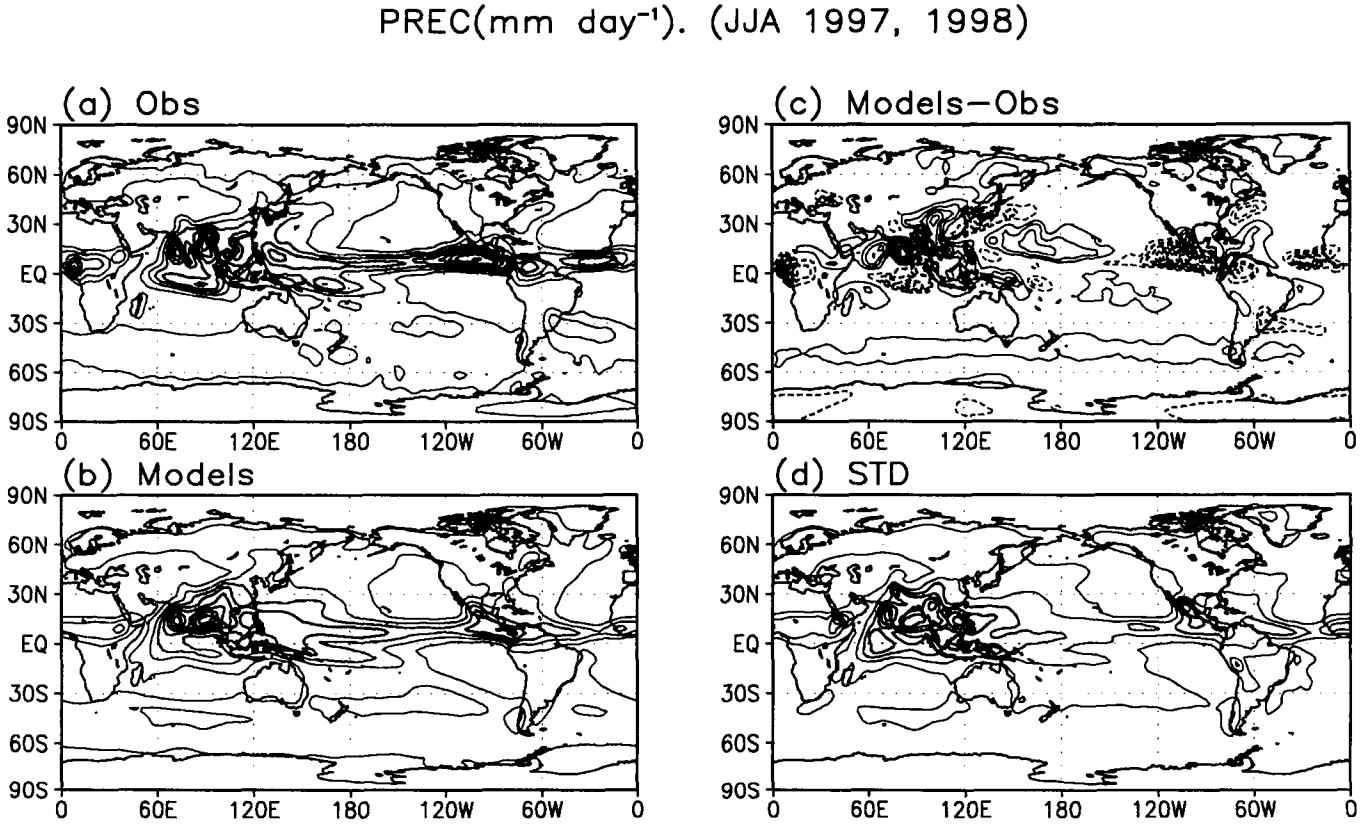
PREC(mm day⁻¹). (JJA 1997, 1998)
(a) Obs
(b) Models
(c) Models−Obs
(d) STD
90N
60N
30N
EQ
30S
60S
90S
0
60E
120E
180
120W
60W
0

Fig.5

(a) Pattern Correlation

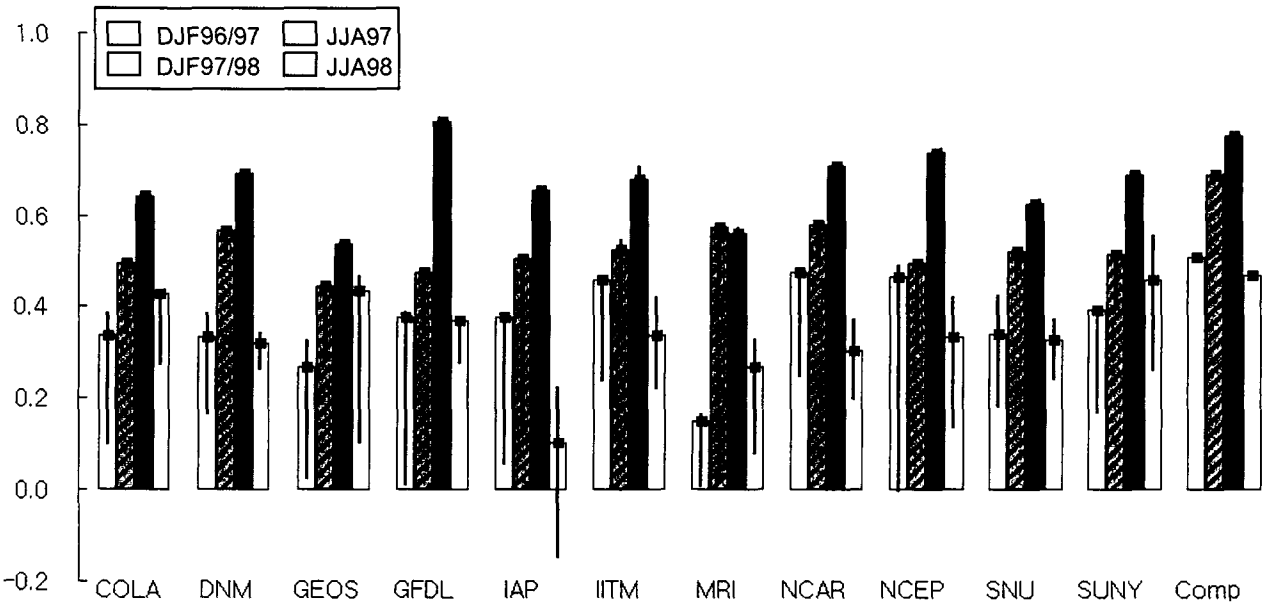

(b) Root-mean-square

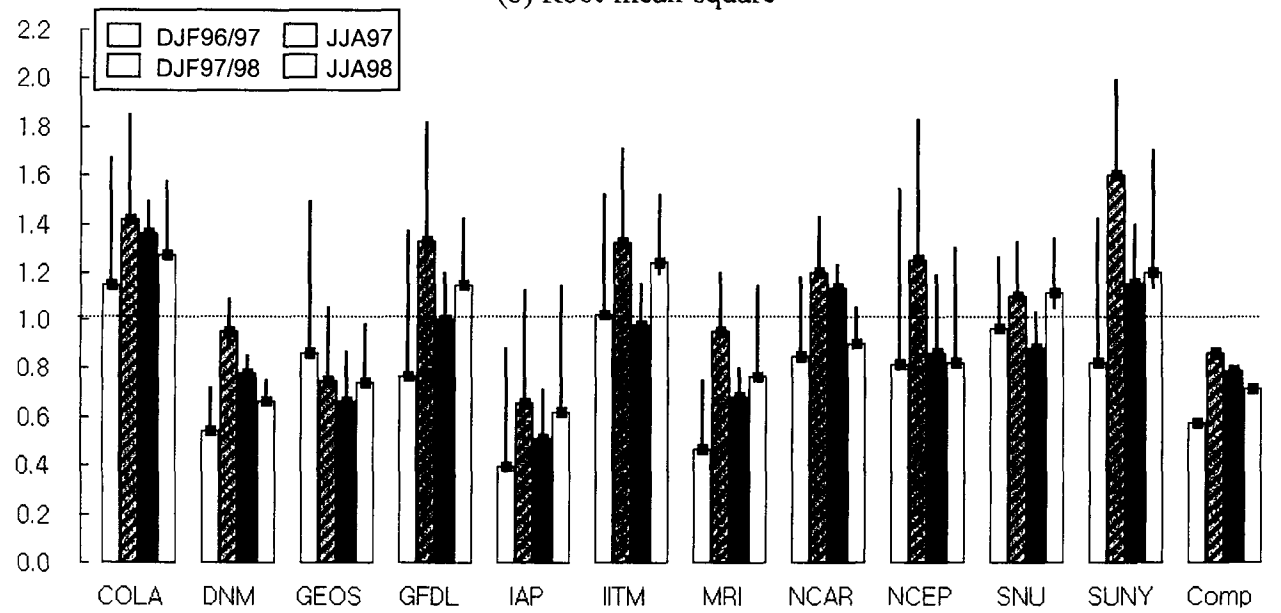

Fig.6

(a) Pattern correlation

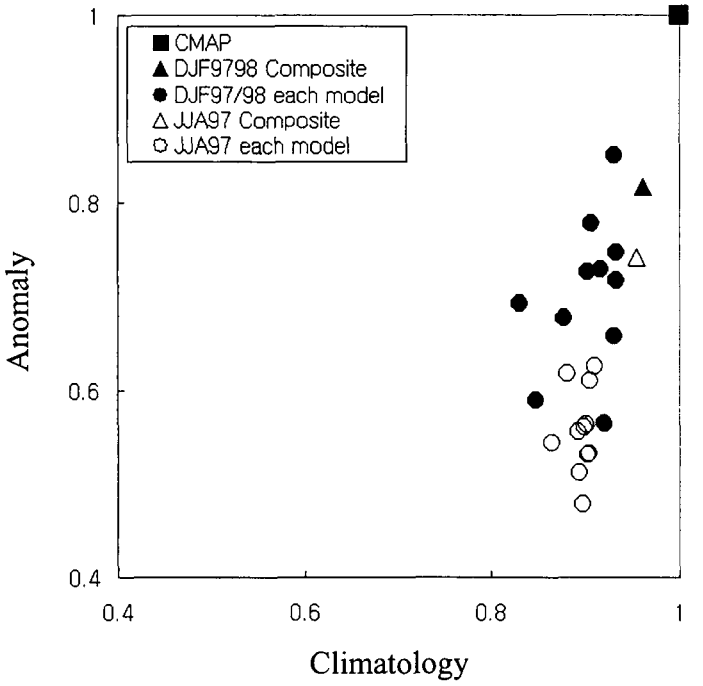

(b) RMS

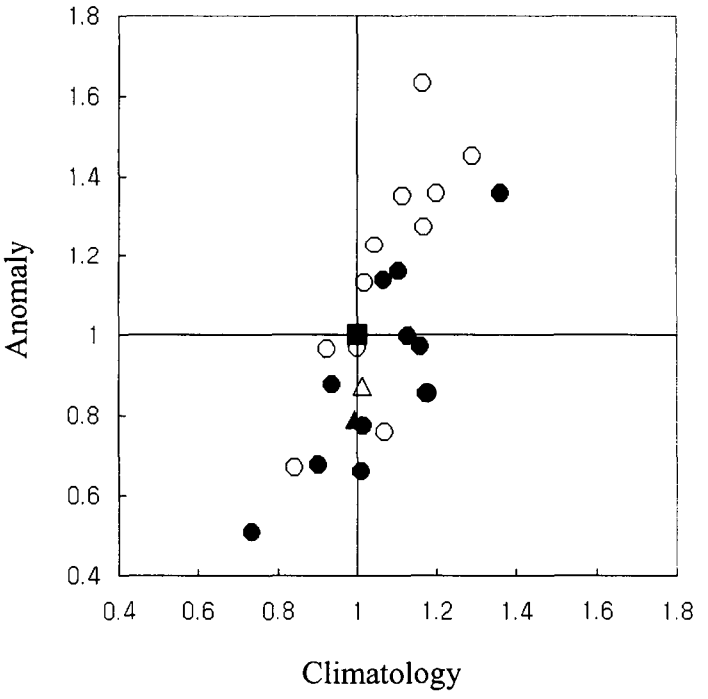

Fig.7

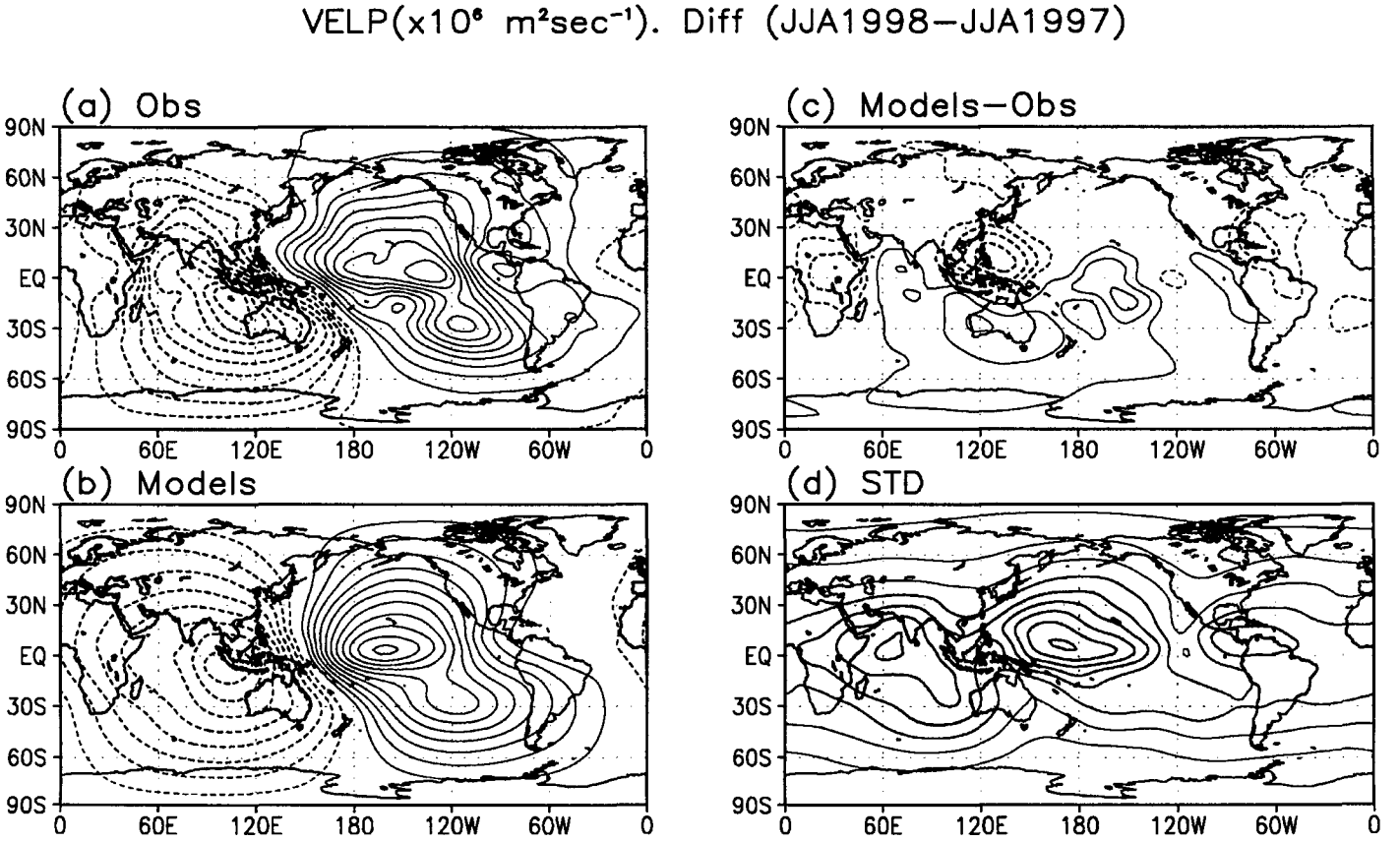
VELP(x10⁶ m²sec⁻¹). Diff (JJA1998−JJA1997)
(a) Obs
(c) Models−Obs
(b) Models
(d) STD
90N
60N
30N
EQ
30S
60S
90S
0
60E
120E
180
120W
60W
0

Fig.8

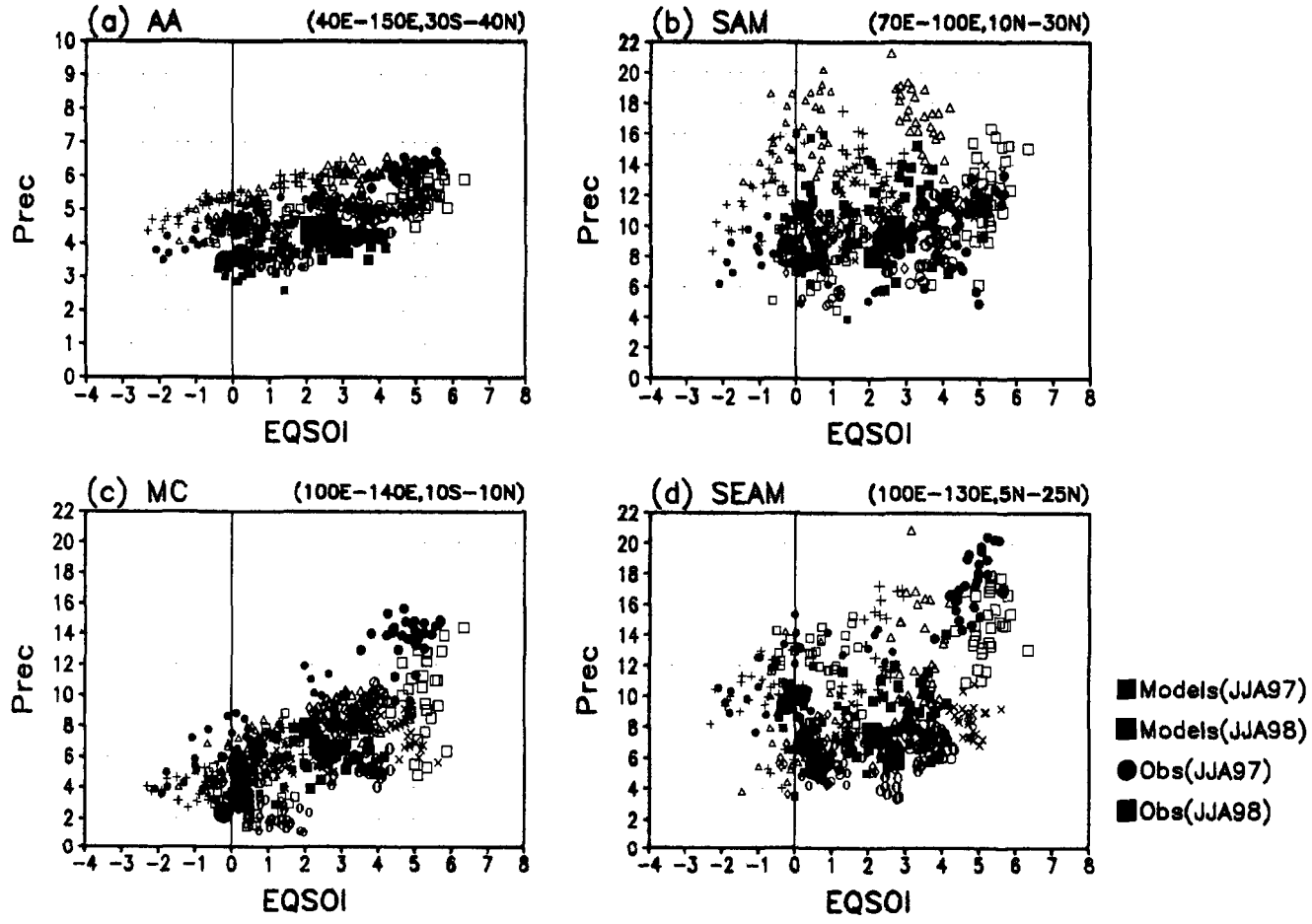
(a) AA
(40E-150E,30S-40N)
(b) SAM
(70E-100E,10N-30N)
(c) MC
(100E-140E,10S-10N)
(d) SEAM
(100E-130E,5N-25N)
Prec
EQSOI
Models(JJA97)
Models(JJA98)
Obs(JJA97)
Obs(JJA98)

Fig.9

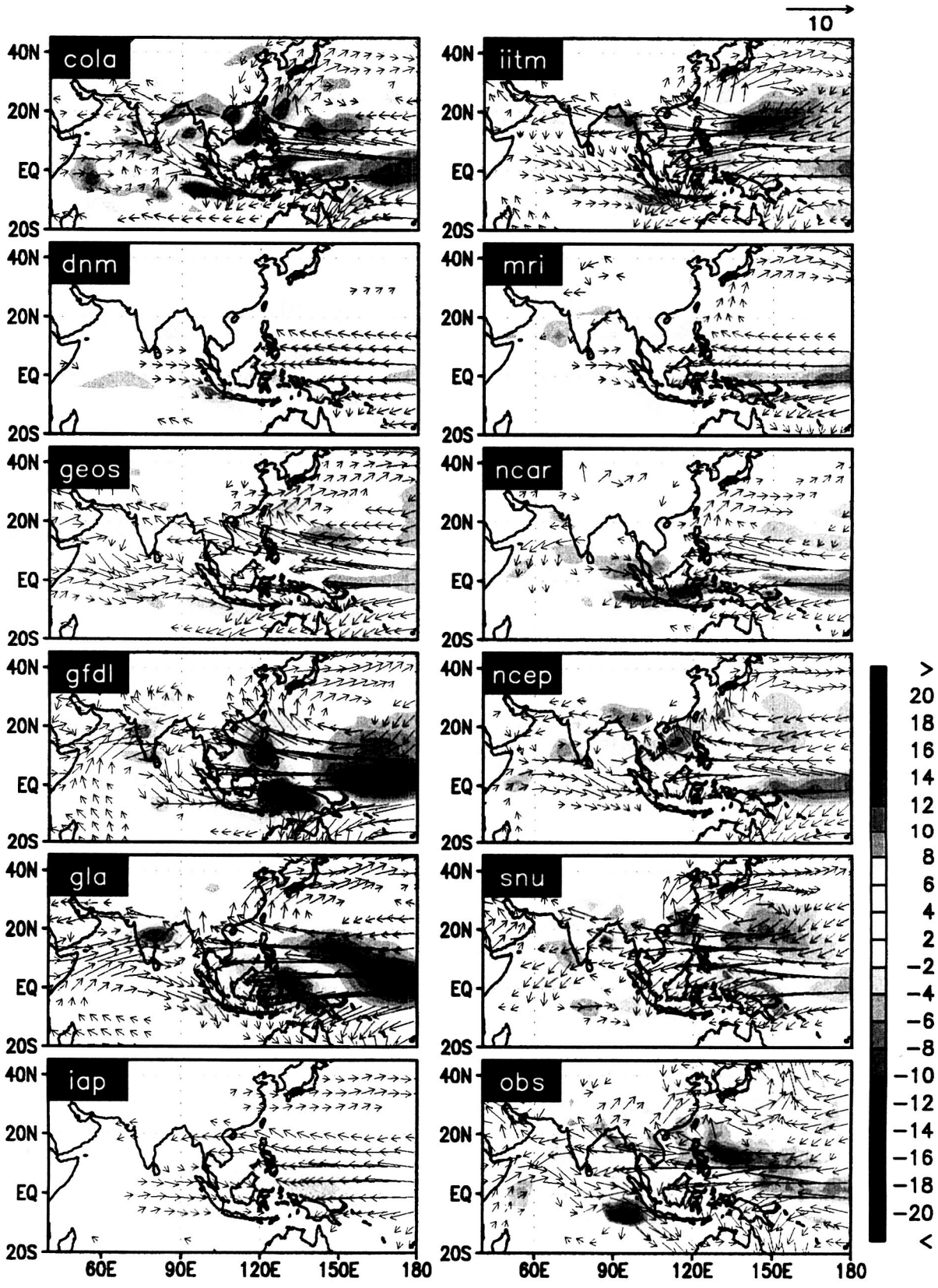
Prec Diff (JJA98−JJA97)
10
cola
iitm
dnm
mri
geos
ncar
gfdl
ncep
gla
snu
iap
obs
40N
20N
EQ
20S
60E
90E
120E
150E
180
>
20
18
16
14
12
10
8
6
4
2
−2
−4
−6
−8
−10
−12
−14
−16
−18
−20
<

Fig.10

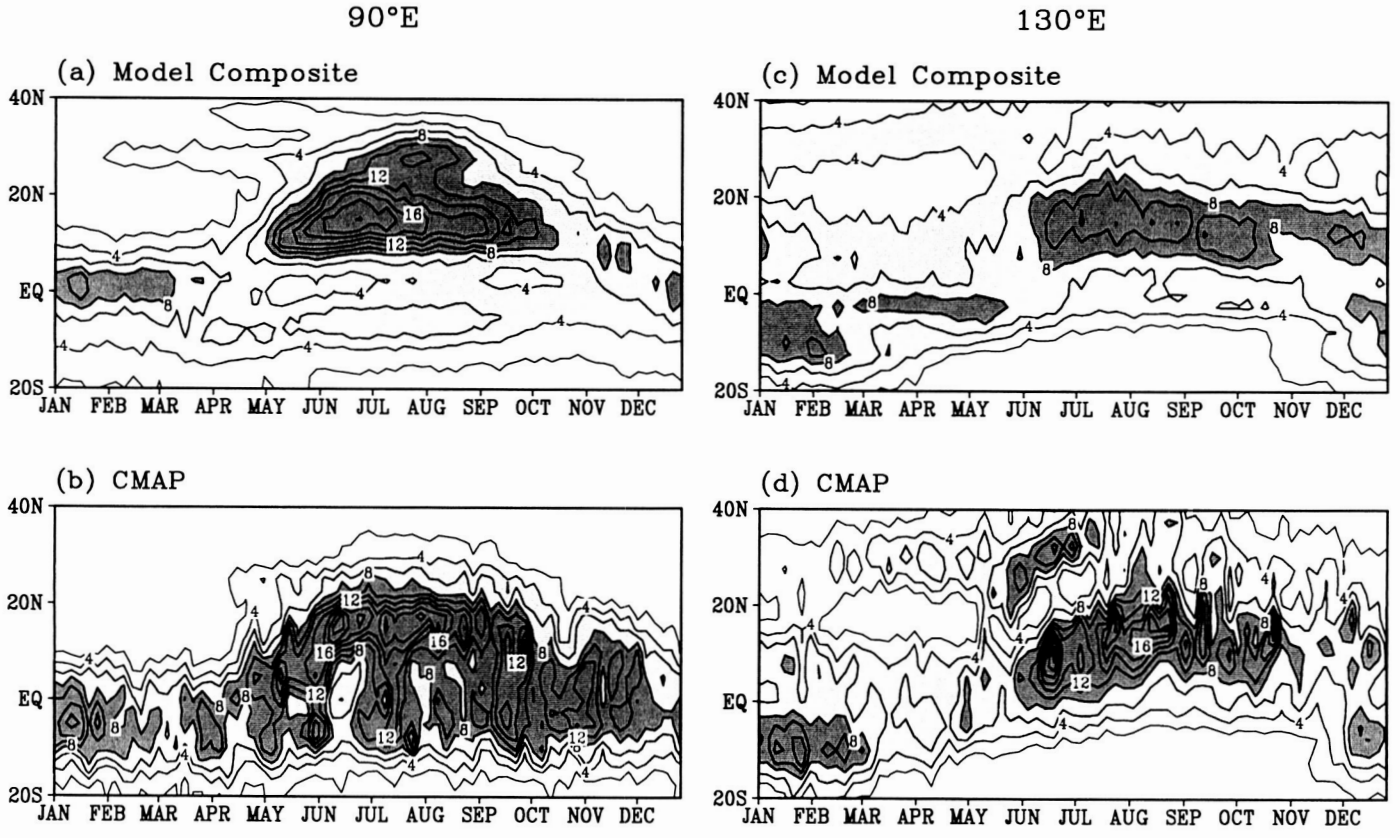
90°E
130°E
(a) Model Composite
(c) Model Composite
(b) CMAP
(d) CMAP
40N
20N
EQ
20S
JAN FEB MAR APR MAY JUN JUL AUG SEP OCT NOV DEC

Fig.11

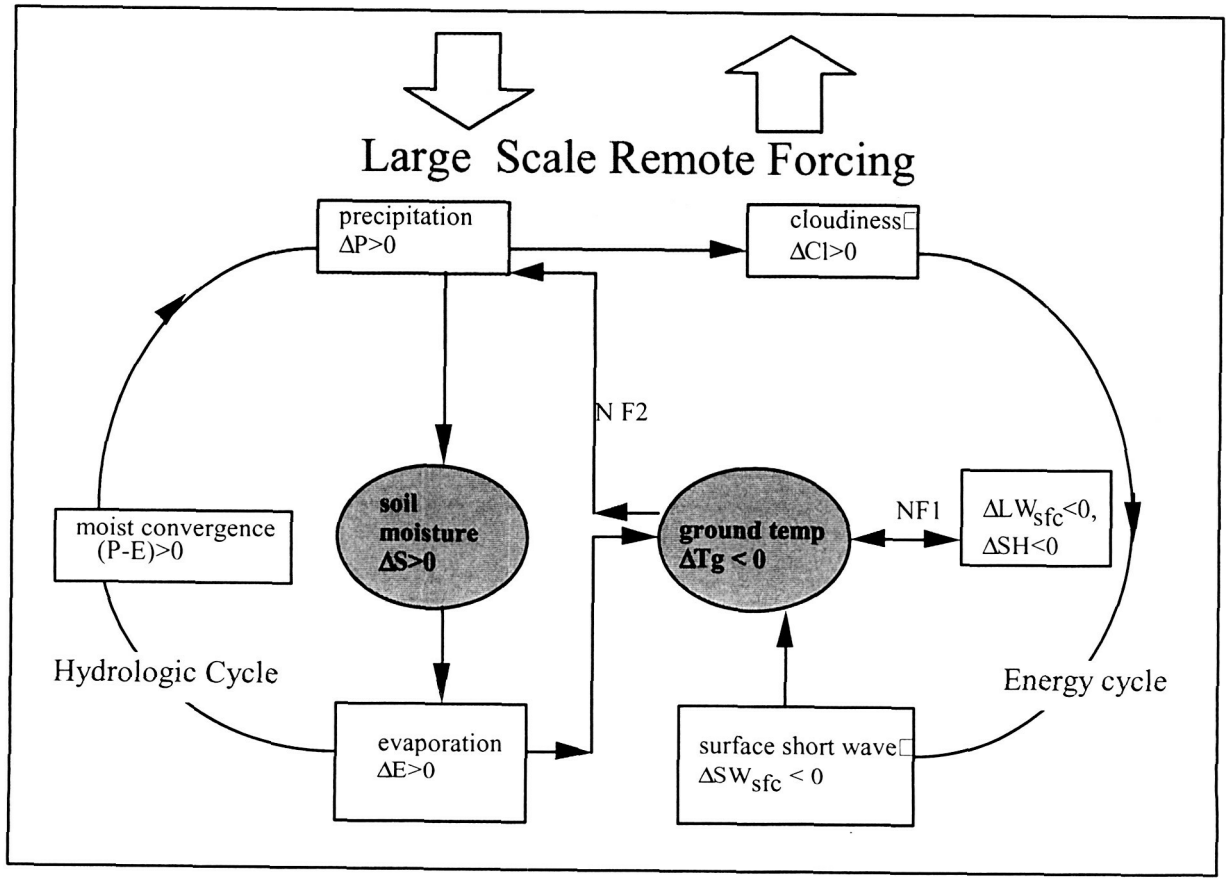
Large Scale Remote Forcing
precipitation
ΔP>0
cloudiness
ΔCl>0
N F2
soil
moisture
ΔS>0
ground temp
ΔTg < 0
NF1
ΔLW$_{sfc}$<0,
ΔSH<0
moist convergence
(P-E)>0
Hydrologic Cycle
Energy cycle
evaporation
ΔE>0
surface short wave
ΔSW$_{sfc}$ < 0

Fig.12

Model interpretation of Climate Signals:
Application to the Asian Monsoon Climate

William K. M. Lau
NASA/Goddard Space Flight Center

Submitted to Cambridge University Press
"The Global Climate System: Patterns, Processes, and Teleconnections"

Popular Summary

This is an invited review paper intended to be published as a Chapter in a book entitled "The Global Climate System: Patterns, Processes and Teleconnections" Cambridge University Press. The author begins with an introduction followed by a primer of climate models, including a description of various modeling strategies and methodologies used for climate diagnostics and predictability studies. Results from the CLIVAR Monsoon Model Intercomparison Project (MMIP) were used to illustrate the application of the strategies to modeling the Asian monsoon. It is shown that state-of-the art atmospheric GCMs have reasonable capability in simulating the seasonal mean large scale monsoon circulation, and response to El Nino. However, most models fail to capture the climatological as well as interannual anomalies of regional scale features of the Asian monsoon. These include in general over-estimating the intensity and/or misplacing the locations of the monsoon convection over the Bay of Bengal, and the zones of heavy rainfall near steep topography of the Indian subcontinent, Indonesia, and Indo-China and the Philippines. The intensity of convection in the equatorial Indian Ocean is generally weaker in models compared to observations. Most important, an endemic problem in all models is the weakness and the lack of definition of the Mei-yu rainbelt of the East Asia, in particular the part of the Mei-yu rainbelt over the East China Sea and southern Japan are under-represented. All models seem to possess certain amount of intraseasonal variability, but the monsoon transitions, such as the onset and breaks are less defined compared with the observed. Evidences are provided that a better simulation of the annual cycle and intraseasonal variability is a pre-requisite for better simulation and better prediction of interannual anomalies.